Journal of Biomolecular NMR, 2 (1992) 149–160
ESCOM

J-Bio NMR 045

Multidimensional ^{1}H and ^{15}N NMR investigation of glutamine-binding protein of *Escherichia coli*

Nico Tjandra, Virgil Simplaceanu, Patricia F. Cottam and Chien Ho*

Department of Biological Sciences, Carnegie Mellon University, 4400 Fifth Avenue, Pittsburgh, PA 15213, U.S.A.

Received 29 July 1991
Accepted 28 August 1991

Keywords: Backbone assignment; 3D NMR; Heteronuclear NMR; NOESY; ^{1}H NMR; ^{15}N NMR; Binding protein

SUMMARY

Specific and uniform ^{15}N labelings along with site-directed mutagenesis of glutamine-binding protein have been utilized to obtain assignments of the His^{156}, Trp^{32} and Trp^{220} residues. These assignments have been made not only to further study the importance of these 3 amino acid residues in protein–ligand and protein–protein interactions associated with the active transport of L-glutamine across the cytoplasmic membrane of *Escherichia coli*, but also to serve as the starting points in the sequence-specific backbone assignment. The assignment of $H_{\varepsilon 2}$ of His^{156} refines the earlier model where this particular proton forms an intermolecular hydrogen bond to the δ-carbonyl of L-glutamine, while assignments of both Trp^{32} and Trp^{220} show the variation in local structures which ensure the specificity in ligand binding and protein–protein interaction. Using 3D NOESY-HMQC NMR, amide connectivities can be traced along 8–9 amino acid residues at a time. This paper illustrates the usefulness of combining ^{15}N isotopic labeling and multinuclear, multidimensional NMR techniques for a structural investigation of a protein with a molecular weight of 25 000.

INTRODUCTION

Understanding the structure and dynamic properties of periplasmic binding proteins is one of the first steps in building a model for a complex membrane transport system. Ames (1986) has proposed a two-step model for active transport. In this model, periplasmic binding proteins play a very important role in transferring a specific ligand to the corresponding membrane protein in an energy-dependent active transport across the cytoplasmic membrane. The glutamine transport system in *Escherichia coli* has been studied extensively (Weiner and Heppel, 1971). It is a single transport system for L-glutamine, containing a glutamine-binding protein (GlnBP) and at least two membrane-associated protein components (Nohno et al., 1986). The dependence of glut-

* To whom correspondence should be addressed.

0925-2738/$ 5.00

amine transport on GlnBP, L-glutamine, as well as pyruvate as an energy source and NAD as a cofactor in the metabolism of pyruvate, has been demonstrated by an in vitro reconstitution of the glutamine transport in a membrane vesicle system (Hunt and Hong, 1981). L-Glutamine is the only naturally occurring amino acid that binds to GlnBP at neutral pH. It has a dissociation constant of 5×10^{-7} M at 5°C and pH 7.2. The protein is stable to changes in pH and temperature (Shen et al., 1989a). GlnBP is a monomeric protein with 256 amino acid residues (molecular weight of about 25000). These characteristics make GlnBP a suitable model for investigating its molecular basis for active transport.

Biochemical and molecular genetic studies have shown the importance of the two tryptophan residues (W32 and W220) in GlnBP for transport activity (Hunt and Hong, 1983; Shen et al., 1989b), while spectroscopic studies have verified both the conformational changes that occur upon ligand binding (Weiner and Heppel, 1971; Kreishman et al., 1973; Shen et al., 1989a) and the formation of an intermolecular hydrogen bond between L-Gln and the GlnBP (Shen et al., 1989a). Determining the structure of GlnBP is a vital step in understanding its properties, such as the ligand-binding mechanism, protein–protein recognition and interaction, and how these specific activities are interconnected through a conformational change as a means of transferring information from one region of the protein to another. Nuclear magnetic resonance (NMR) is a powerful tool for probing both the structure and dynamics of proteins in solution (Jardetzky and Roberts, 1981; Wagner, 1983; Wüthrich, 1986).

The challenge in elucidating the structure of GlnBP, from the NMR point of view, is the assignment of particular resonances. Conventional 1D and 2D homonuclear ^{1}H NMR spectroscopies give very little aid in this case due to the size of the protein molecule. Using heteronuclear 2- and 3D NMR, where ^{1}H-^{1}H scalar coupling is not relied upon, plus uniform and selective isotopic labelings, ^{1}H resonance assignments of GlnBP protein can be achieved. This paper illustrates the use of ^{15}N uniformly and selectively labeled GlnBP along with heteronuclear, multiple quantum correlation spectroscopy (HMQC) (Mueller, 1979; Bax et al., 1983; Bendall et al., 1983), nuclear Overhauser and exchange spectroscopy (NOESY)-HMQC NMR (Gronenborn et al., 1989; Marion et al., 1989a,b; Driscoll et al., 1990) to obtain ^{1}H resonance assignments.

MATERIALS AND METHODS

Sample preparation

GlnBP was purified from cultures of *E. coli* K12 (ATCC#10798) or W3110*trp*A33 (Drapeau et al., 1968) following transformation with plasmids pGT1-2 and pJW133. Plasmid pJW133 was constructed by Dr. J.-S. Hong from pT7-5 (Tabor and Richardson, 1985). It carries an *Eco*RI fragment of the glutamine transport operon. Plasmids pGT1-2 and pJW133 were gifts from Dr. Hong. W3110*trp*A33 was the gift of Dr. C. Yanofsky.

^{15}N Selectively labeled GlnBP from *E. coli* W3110*trp*A33 was grown in a medium composed of 1.0% casamino acids (Difco), 0.2% glucose, 0.06 M potassium phosphate buffer at pH 7.0, 0.1%

Abbreviations: NOE, nuclear Overhauser effect; NOESY, nuclear Overhauser enhancement spectroscopy; HMQC, heteronuclear multiple quantum coherence spectroscopy; NMR, nuclear magnetic resonance; GlnBP, glutamine binding protein; L-Gln (or N), L-glutamine; His (or H), L-histidine; Trp (or W), L-tryptophan, EDTA, ethylenediamine tetraacetic acid; S/N, signal-to-noise.

$(NH_4)_2SO_4$ and 0.01% $MgSO_4 \cdot 7H_2O$. [Indole-$^{15}N_1$]L-tryptophan and [ring-1,3-$^{15}N_2$]L-histidine (which were gifts from the National Stable Isotopes Resources at Los Alamos), ^{15}N-α-histidine (Cambridge Isotope), and ^{15}N-α-tryptophan (Merck) were supplied at a final concentration of 20 μg/ml.

^{15}N Uniformly labeled GlnBP was obtained from *E. coli* K12 grown in minimal 0.4% glucose with 0.07–0.10% $(^{15}NH_4)_2SO_4$ as the sole source of nitrogen. Fifty μg/ml kanamycin and ampicillin were included in all media.

All cells were grown overnight at 30–32°C with aeration until they reached stationary state and then shifted to 42°C and rifampicin was added to induce exclusive GlnBP production (Tabor and Richardson, 1985). GlnBP was extracted from the cells by chloroform-shock treatment (Ames et al., 1984), and purified using the procedure developed in our laboratory (Shen et al., 1989a). Because of the high affinity of GlnBP towards its substrate, it usually contains bound L-Gln throughout the purification procedure. Ligand-free GlnBP was obtained by first denaturing the protein in 6 M guanidine–HCl at 5°C and then renaturing it by dialyzing against 10 mM Tris–HCl at pH 7.6 (or 10 mM potassium phosphate at pH 7.2), containing 0.1 mM K_2EDTA. The protein was then repurified using the usual procedure mentioned above. The recovery of ligand-free GlnBP after denaturing was usually 50%. All NMR samples contain 3.5–6 mM protein in 100 mM potassium phosphate at pH 7.2 and 10% ^2H_2O with or without 20 mM L-Gln.

NMR spectroscopy

NMR experiments were carried out at 27°C on a Bruker AM-500 spectrometer equipped with a broadband double resonance reverse-probe optimized for ^{1}H detection. NOESY-HMQC spectra were recorded with 32 complex data points in t_2, while quadrature and States detections (States et al., 1982) were used to obtain 256 complex points in the t_3 and t_1 dimensions, respectively. With 32 scans per complex pair (t_1,t_3) and a 1-s relaxation delay, the experiment takes 3.5 days to obtain a typical signal-to-noise (S/N) ratio in the amide region of ~20 and in the aliphatic region of ~80. Processing data in the t_2 dimension was done using the Omega2 software provided to us by Dr. John L. Markley at the National Magnetic Resonance Facility at Madison, WI, while processing in the t_1 and t_3 dimensions was done on an ASPECT-3000 computer using DISNMR89 software from Bruker. A shifted-squared sinebell window and zero filling of the data were used in the t_3 domain, and a doubly shifted-squared sinebell window and zero filling were used in the t_1 domain. The NOE mixing time was 120 ms to show the spin diffusion problem in this protein. The HMQC spectra were recorded with a maximized 4.5-ms refocusing delay, ^{15}N decoupling during acquisition was not used. In the t_1 dimension, 256 complex data points were acquired, while 1024 complex points were sampled during acquisition. Data were processed on an ASPECT-3000 computer, with a sinebell window and zero filling in both dimensions. A relaxation delay of 1 s per scan and 128 scans per (t_1,t_2) pair was used to give a typical S/N of ~60. 1D ^{1}H NMR spectra were recorded using a jump-and-return pulse sequence (Plateau et al., 1983) with a 55-μs delay between the two 90° pulses and post-processing for water signal correction. The ^{15}N NMR spectra were taken with ^{1}H decoupling during acquisition and a 5-s relaxation delay to minimize NOE. The ^{1}H and ^{15}N chemical shifts are referenced to DSS at 0 ppm and to $^{15}NH_4NO_3$ at 24 ppm, respectively. Chemical shifts are estimated to within ± 0.01 ppm and ± 0.2 ppm for ^{1}H and ^{15}N, respectively, in 1D spectra.

RESULTS AND DISCUSSION

The differences in the 1D ^{1}H NMR spectra of GlnBP and the GlnBP–Gln complex (Figs. 1A,B) can easily be seen in the exchangeable region (10–15 ppm from DSS) and the ring-current shifted region (0 to −1 ppm), which illustrate that some specific conformational changes result from ligand binding. These changes are believed to be a major factor in the ability of the membrane–protein complex to recognize and bind the ligand carrier, resulting in a very efficient transport mechanism. It has been pointed out that these exchangeable resonances arise from intermolecular and intramolecular hydrogen bonds (Shen et al., 1989a). The resonance at 11.6 ppm (Fig. 1B) has been assigned by using ^{15}N-labeled histidine and an HMQC experiment to be the $H_{\varepsilon 2}$ of the only histidine residue at position 156 (Fig. 2). The resonance at 11.03 ppm in the spectrum of the GlnBP–Gln complex or 11.14 ppm in the spectrum of GlnBP has been assigned using site-directed mutagenesis to the N_1H of W220 (Shen et al., 1989a), and has been confirmed by using ^{15}N-indole-labeled tryptophan and an HMQC experiment (Fig. 3). From the same experiment, N_1H of W32 has been assigned to the resonance at $\delta_{1H} = 5.81$ ppm. The same spectrum shows a typical

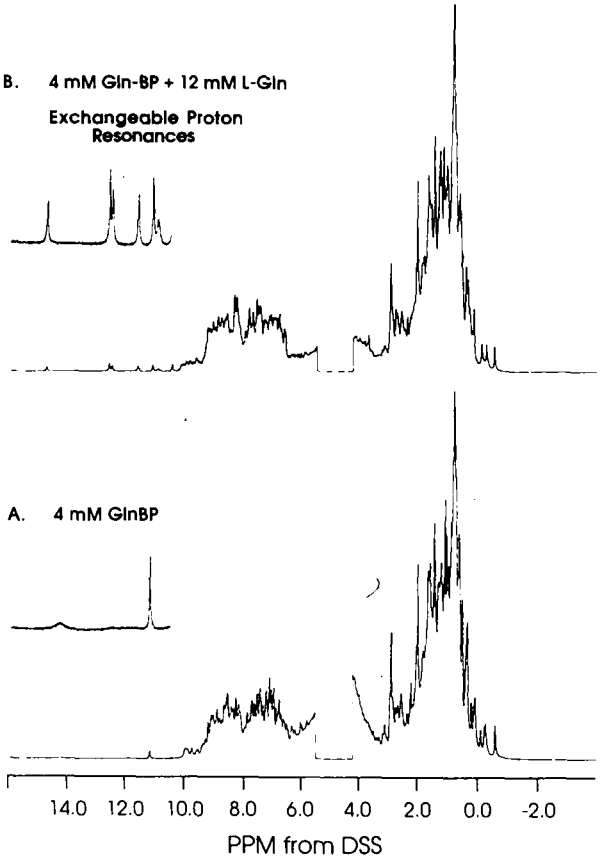

Fig. 1. 500 MHz ^{1}H NMR spectra of 4 mM GlnBP in 100 mM potassium phosphate in H_2O at pH 7.2 and 29°C: (A) in the absence of L-glutamine; and (B) in the presence of 12 mM L-glutamine. The exchangeable proton resonance region is expanded to show conformational change upon substrate binding.

^{1}H natural linewidth of greater than 10 Hz for this protein at 500 MHz, compared to a ^{1}H-^{1}H scalar coupling of 2–8 Hz.

^{15}N NMR spectra also indicate that conformational changes occur upon ligand binding (Figs. 4A,B). The resonances at 170 ppm and 248 ppm in the spectrum of the GlnBP–Gln complex were assigned to $H156_{\varepsilon 2}$ and $H156_{\delta 1}$ based on their chemical shifts, and have been confirmed by using ^{15}N-labeled histidine (Fig. 2). In the absence of L-glutamine, these two lines are broad. This could be due to an exchange process or restricted local mobility in the GlnBP molecule.

All of the assignments made so far are shown in the 2D HMQC spectra of both the GlnBP and GlnBP–Gln complex (Figs. 5A,B). The doublets in the ^{1}H dimension which are seen in these spectra are due to scalar coupling to ^{15}N since no ^{15}N decoupling was used during acquisition in order to help distinguish the signal from the noise. All of the above mentioned spectra illustrate the problem with overlapping resonances. Even though the 2D HMQC spectra show very little resolution to aid in assignment, a solution to this problem is to use selective labeling, along with site-directed mutagenesis. This is illustrated in Figs. 6A and B, where ^{15}N-α-tryptophan was used to label wild-type GlnBP as well as a mutant GlnBP ($Trp^{220} \rightarrow Phe$). Replacement of W220 with Phe results in the disappearance of the resonance at 7.12 ppm (Fig. 6B). The assignment of the amide protons for these Trps is trivial, since there are only two Trp residues in the protein; however, as the number of residues increases, the assignment becomes more difficult. The results obtained so far will be used as starting points in the sequential assignment.

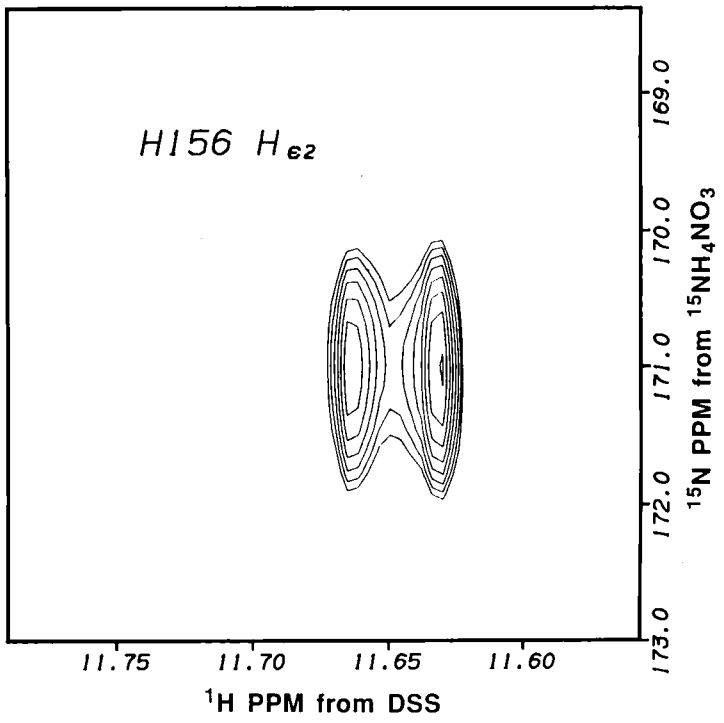

Fig. 2. 11.7 Tesla 2D HMQC ^{15}N-^{1}H spectrum of 3.5 mM [ring-1,3-$^{15}N_2$]His-labeled GlnBP + 10 mM L-glutamine in 100 mM potassium phosphate in H_2O at pH 7.2 and 29° C. ^{15}N decoupling during acquisition was not used. Only one peak was observed, which is $H156_{\varepsilon 2}$.

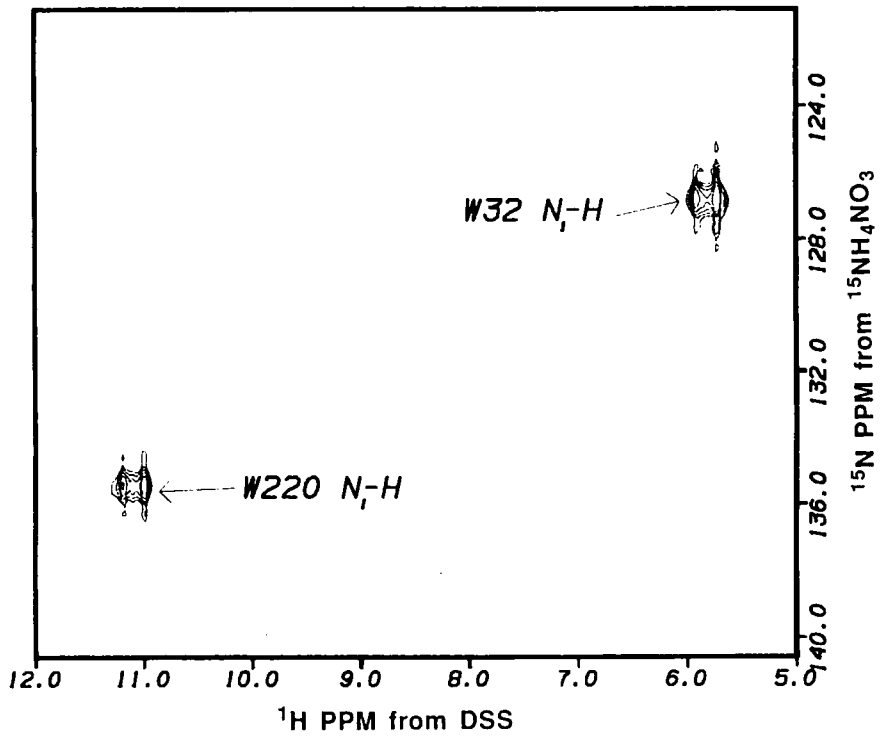

Fig. 3. 11.7 Tesla 2D HMQC ^{15}N-^{1}H spectrum of 4 mM [indole-$^{15}N_1$]Trp-labeled GlnBP + 10 mM L-glutamine in 100 mM potassium phosphate in H_2O at pH 7.2 and 29 °C. Both N_1-H of W32 and W220 are shown.

The second solution in aiding assignment is to use a 3D NOESY-HMQC experiment, where the large ^{1}H-^{15}N scalar coupling is utilized to separate the amide resonances with their ^{15}N chemical shifts. A slice taken along the ^{15}N dimension at 126.60 ppm (Fig. 7A) shows NOEs from the amide proton of H156 to its α-, β- and other aliphatic protons, and from N_1H of W32 to some aromatic as well as some aliphatic protons. Similarly, a slice taken at 135.55 ppm (Fig. 7B) shows NOEs from N_1H of W220. Spin diffusion can easily be observed at 120-ms mixing time in the aliphatic region. Both W32α and W220α are easily observed in the 3D NOESY-HMQC spectra (Figs. 8A,B), while β-protons are not very well resolved, due to the large number of β- and γ-protons and of spin diffusion. The overlap of peaks in the amide region has been reduced substantially. This fact makes it possible to do a limited sequential assignment based on the NH-NH connectivities.

Using the amide of W32 as a starting point, one can see its connectivity (Fig. 9). A slice taken at $\delta_{15N} = 121.48$ ppm shows the starting point and the NOE peak of amide W32 to the amide of A1 (W32, A1) and (W32, B1). The A and B labels have been used because the direction of connectivity along the sequence is still unknown. The slice at $\delta_{15N} = 122.12$ ppm shows the complementary NOE peak to the previous slice, namely (B1, W32), while the slice at $\delta_{15N} = 113.81$ ppm indicates (A1, W32), as well as the next connectivity (A1, A2). The final slice taken at $\delta_{15N} = 120.85$ ppm points out the complementary NOE (A2, A1) and the next step (A2, A3). Similarly, using the amide of W220 as a starting point one can observe another network of connectivities (Fig. 10). Again, the direction has not been determined.

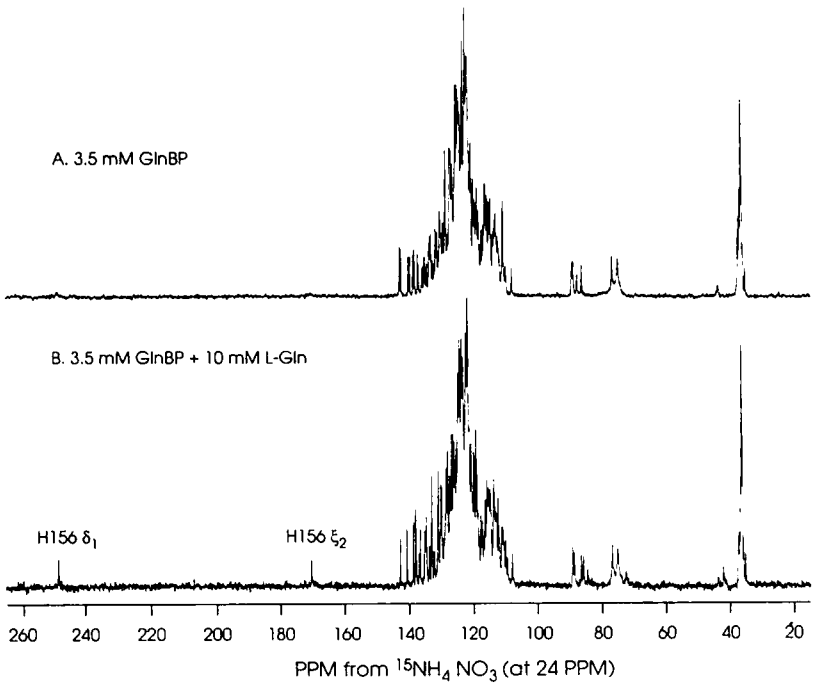

Fig. 4. 50.68 MHz ^{15}N NMR spectra of 3.5 mM uniformly ^{15}N-labeled GlnBP in 100 mM potassium phosphate in H_2O at pH 7.2 and 29 C: (A) in the absence of L-glutamine, the resonances at 171 and 240 ppm are broad; and (B) in the presence of 10 mM L-glutamine, the $H156_{\delta 1}$ and $H156_{\epsilon 2}$ peaks become sharper and observable.

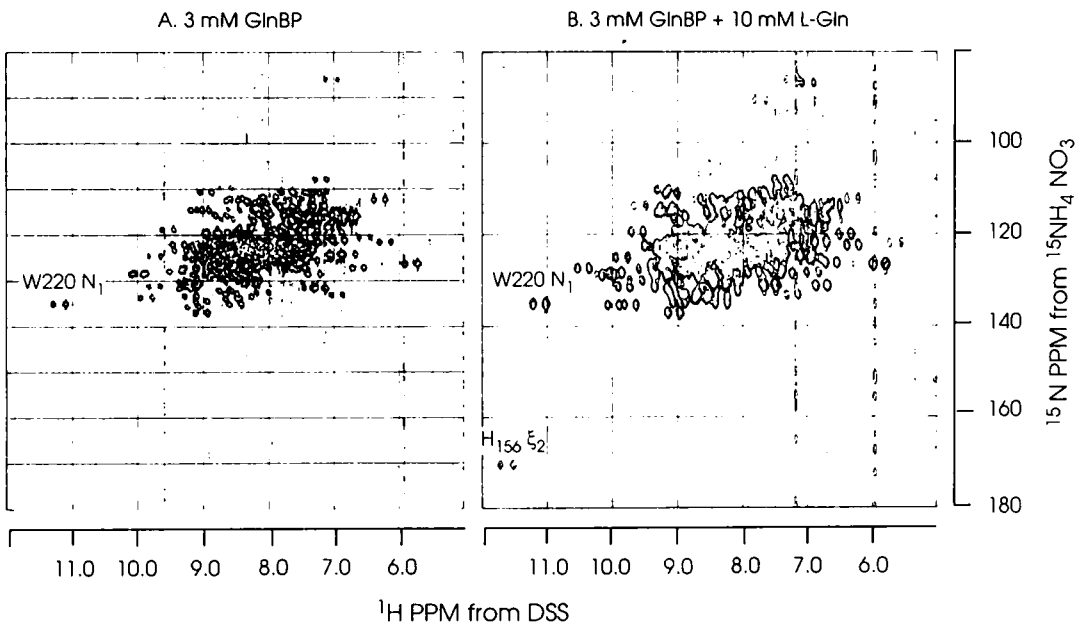

Fig. 5. 11.7 Tesla 2D HMQC ^{15}N-^{1}H spectra of ^{15}N-uniformly labeled GlnBP in 100 mM potassium phosphate in H_2O at pH 7.2 and 29 C: (A) in the absence of L-Gln; and (B) in the presence of 10 mM L-Gln. ^{15}N decoupling during acquisition was not used.

The histidine (H156) and two tryptophans (W32 and W220) have been chosen for assignment not only because they occur in the smallest number in the GlnBP molecule, but they are also believed to be among the most important amino acid residues in ligand binding and protein–protein interaction (Shen et al., 1989a,b). The assignment of the indole N_1-H of both tryptophans complements results obtained by Shen et al. (1989b). The indole N_1-H of W32 is shifted upfield indicating that it is close to an aromatic-ring structure (Phe or Tyr), and possibly buried within the protein (Shen et al., 1989b), while the indole N_1-H of W220 forms a hydrogen bond to another part of the protein, thus slowing down the exchange of this particular proton with the solvent. The assignment of the $H_{\varepsilon 2}$ of H156 at 11.6 ppm along with earlier results (Shen et al., 1989a) provides a model for the binding site, where the $H_{\varepsilon 2}$ of H156 is hydrogen-bonded to the δ-carbonyl of L-Gln. The formation of an intermolecular hydrogen bond between L-Gln and $H_{\varepsilon 2}$ of H156 may be significant in determining the specificity of ligand binding. Furthermore, the ^{15}N-^{1}H HMQC spectra do not show that any proton is correlated with the $N_{\delta 1}$ of H156, which could mean that the $N_{\delta 1}$ of H156 is not protonated or that it exchanges rapidly with the solvent. In either case, it indicates that the two sides of the H156 imidazole ring are in different environments. All the above properties ensure a specific conformation of the protein–ligand complex, which is required for recogni-

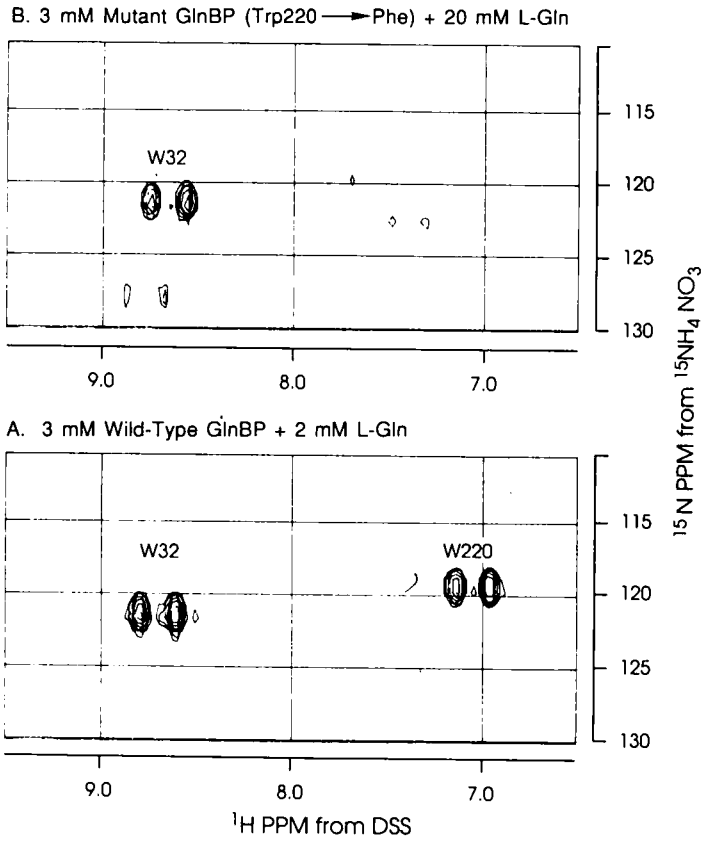

Fig. 6. 11.7 Tesla 2D HMQC spectra of 4 mM ^{15}N-α-Trp-labeled GlnBP in the presence of L-Gln in 100 mM potassium phosphate in H_2O at pH 7.2 and 29 C: (A) wild-type GlnBP shows both amides of W220 and W32; and (B) mutant GlnBP (W220→Phe) shows only amide of W32.

tion by the corresponding membrane proteins in order to complete the translocation step in the transport mechanism.

The assignment of backbone amide protons for W32, W220, and H156 provides starting points for a sequential assignment. In the NOESY-HMQC spectra, connectivities can only be traced along 8–9 residues, when using W32 or W220 as starting points, while H156 is not useful as it does not have any NOE to the next amide protons in the sequence. This could be due to the secondary structure of the protein, for example, short spans of α-helices separated by β-pleated sheets. For a β-sheet structure, the observed NOE is limited to that occurring between H_α and its amide proton, while other ^1H-^1H distances are too long to be obtained by NOE, due to the stretching of the polypeptide chain (Wüthrich, 1986). This result is consistent with the model that has been proposed thus far. Periplasmic binding proteins with specific affinities for sugars, ions, or amino acids contain two globular domain structures, each constructed of a main β-sheet column flanked by short sections of α-helices, while the ligand-binding site is in the bend between the two domains (Gilliland and Quiocho, 1981; Saper and Quiocho, 1983; Quiocho and Vyas, 1984; Pflugrath and Quiocho, 1988). The direction of the assignment has not been established since the sequential connectivity is not long enough to give more information on specific structural features of the protein molecule, such as the location of the mobile carboxy or amino terminal. Additionally, spin system

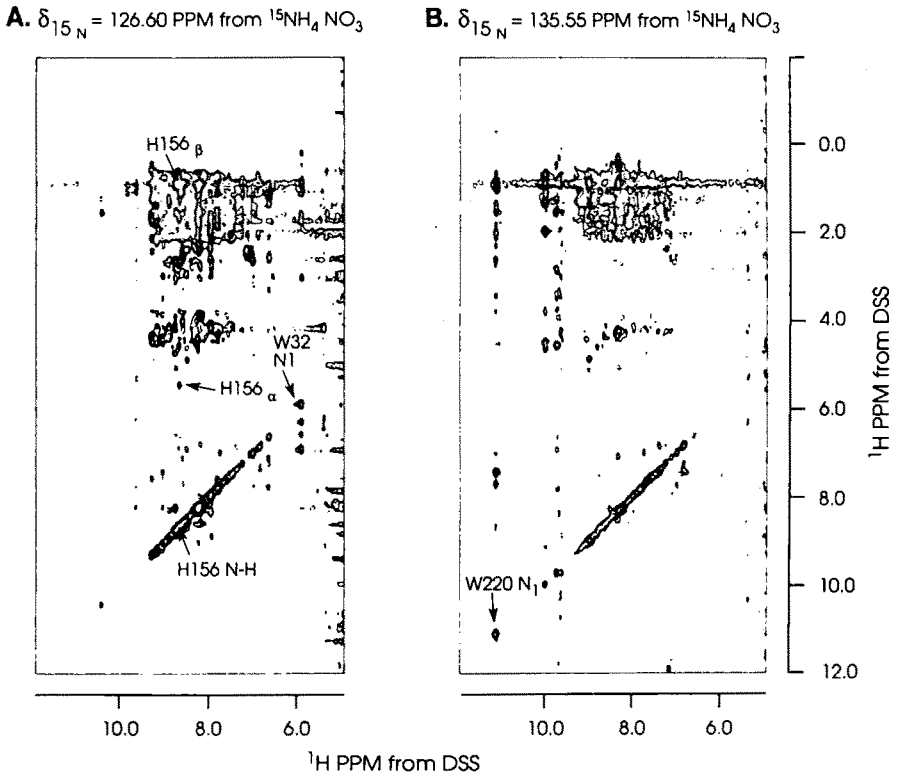

Fig. 7. 11.7 Tesla 3D NOESY-HMQC spectra of 6 mM ^{15}N-uniformly labeled GlnBP + 20 mM L-Gln in 100 mM potassium phosphate in H_2O at pH 7.2 and 29°C. Mixing time of 120 ms: (A) slice taken at δ_{15N} = 126.60 ppm to show NOEs to H156 N-H as well as to W32 N_1-H; and (B) slice taken at δ_{15N} = 135.55 ppm to show NOEs to W220 N_1-H.

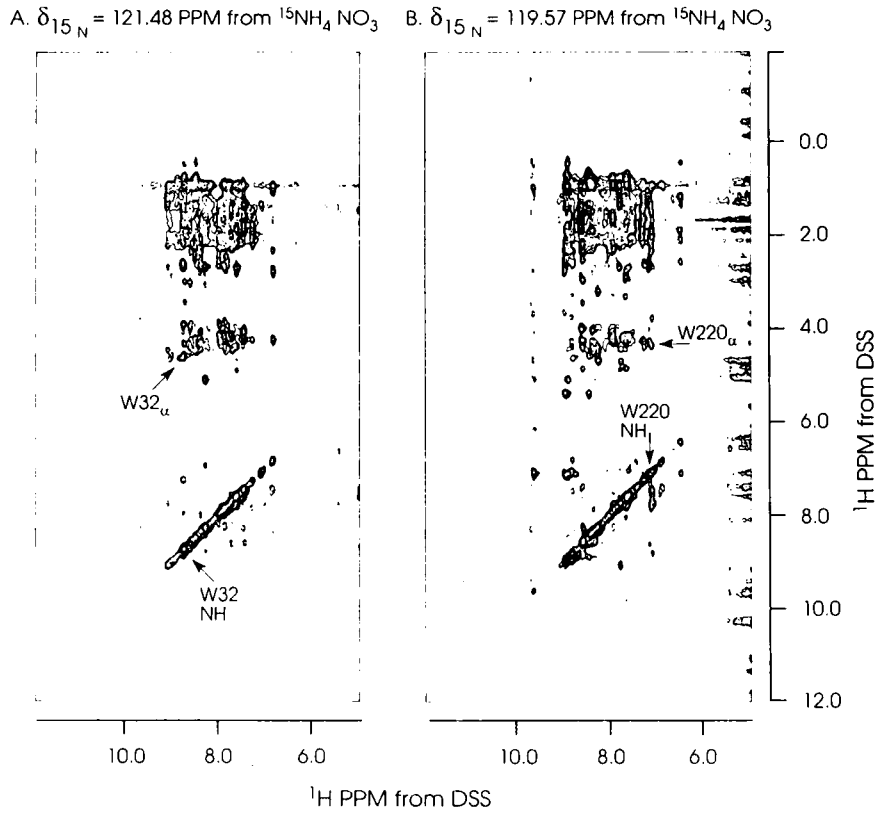

Fig. 8. 11.7 Tesla 3D NOESY-HMQC spectra of 6 mM ^{15}N-uniformly labeled GlnBP + 20 mM L-Gln in 100 mM potassium phosphate in H_2O at pH 7.2 and 29 C. Mixing time of 120 ms: (A) slice taken at δ_{15_N} = 121.48 ppm to show NOEs to amide of W32; and (B) slice taken at δ_{15_N} = 119.57 ppm to show NOEs to amide of W220. Both will be used as starting points in sequential assignment.

information cannot be obtained with a protein of this size, when one relies solely on ^{1}H-^{1}H scalar coupling. This type of information can only be found in a high ^{13}C enrichment of the protein, where one can take advantage of the larger ^{13}C-^{13}C scalar coupling (Oh et al., 1988; Westler et al., 1988).

CONCLUSION

This paper shows both the advantages and difficulties of using 2D HMQC and 3D NOESY-HMQC NMR along with uniform or selective labeling and site-directed mutagenesis to assign resonances for GlnBP, which is the first step in studying its structure and dynamic properties. In the case of 2D HMQC NMR, a large ^{1}H-^{15}N scalar coupling provides an excellent ^{1}H spectrum editing tool. Because of the size and perhaps the compactness of the protein only a few isolated peaks can be obtained. On the other hand, 3D NOESY-HMQC NMR spectroscopy spreads out the ^{1}H 2D NOESY spectrum by using the ^{15}N chemical shifts to simplify substantially the region of interest, namely that of the backbone amide protons. The dependence of 3D NOESY-HMQC NMR on the secondary structure of the protein (Kay et al., 1990), however, limits our ability to completely assign the resonances. Perhaps, using only ^{1}H-^{15}N, ^{1}H-$^{13}C_\alpha$, ^{15}N-$^{13}C_\alpha$ and ^{15}N-^{13}C' scalar couplings in heteronuclear 3D NMR (Ikura et al., 1990; Kay et al., 1990; Montelione and

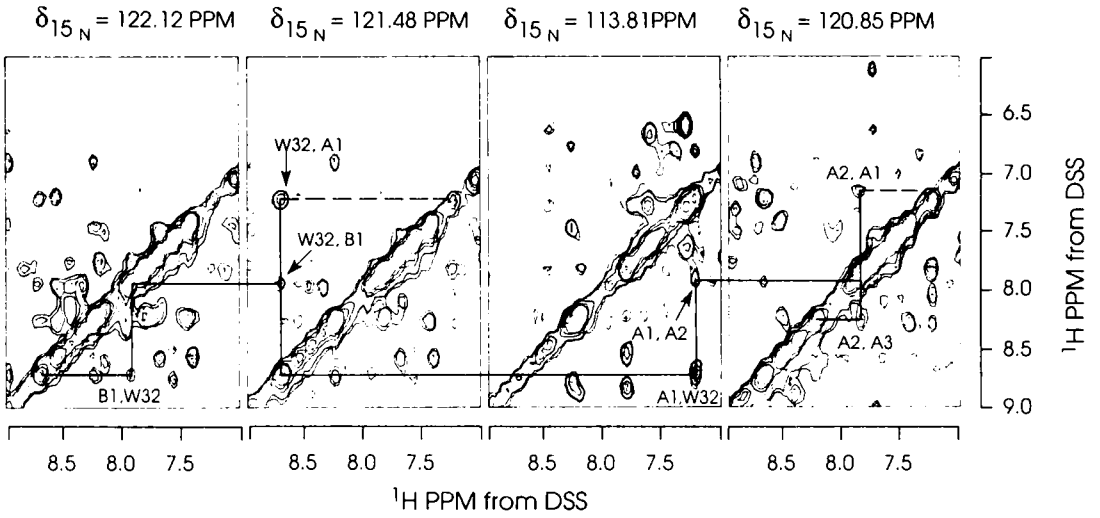

Fig. 9. 11.7 Tesla 3D NOESY-HMQC spectra of 6 mM ^{15}N-uniformly labeled GlnBP + 20 mM L-Gln in 100 mM potassium phosphate in H_2O at pH 7.2 and 29 C. Mixing time of 120 ms. Amide regions were expanded to show backbone connectivity with amide of W32 as starting point, but the direction of connectivity has not been determined, i.e., N_i-N_{i+1} or N_i-N_{i-1}.

Wagner, 1990), and 4D NMR (Clore et al., 1991) to obtain backbone connectivity can solve this problem. Caution certainly must be used since for proteins in this molecular weight range, the ^{15}N linewidths measured from isolated peaks in the 1D ^{15}N NMR spectrum (Figs. 2A,B) range from 10 to 20 Hz, which is comparable, if not larger, to the one-bond ^{15}N-$^{13}C_\alpha$ coupling of 7–11 Hz (Bystrov, 1976). This will certainly lower the sensitivity of the above mentioned heteronuclear 3D NMR techniques which rely on magnetization transfer through one-bond $J_{N,C\alpha}$ coupling (Ikura et

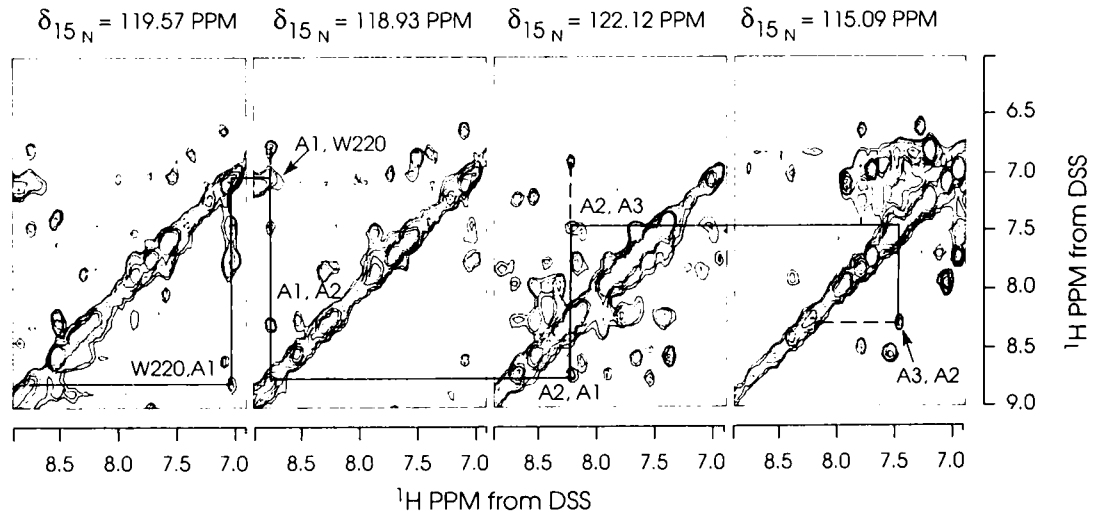

Fig. 10. 11.7 Tesla 3D NOESY-HMQC spectra of 6 mM ^{15}N-uniformly labeled GlnBP + 20 mM L-Gln in 100 mM potassium phosphate in H_2O at pH 7.2 and 29 C. Mixing time of 120 ms. Amide regions were expanded to show backbone connectivity with amide W220 as starting point, but the direction of connectivity has not been determined, i.e., N_i-N_{i+1} or N_i-N_{i-1}.

al., 1990; Kay et al., 1990). This may be overcome by longer signal averaging at higher temperature and/or higher sample concentration. Thus, using heteronuclear 3D NMR and 4D NMR combined with uniform and selective isotopic labelings, the assignment of ^1H resonances can be completed.

ACKNOWLEDGEMENTS

All 3D NMR spectra were processed using the OMEGA2 software which was kindly provided to us by Dr. John L. Markley of the National Magnetic Resonance Facility at the University of Wisconsin. [Indole-$^{15}N_1$]L-tryptophan and [ring-1,3-$^{15}N_2$]L-histidine were kindly given to us by the National Stable Isotopes Resources at Los Alamos. We thank Dr. Susan R. Dowd for helpful discussions. This work is supported by research grants from the National Science Foundation (DMB-8816384) and the National Institutes of Health (GM-26874).

REFERENCES

Ames, G.F.-L. (1986) *Annu. Rev. Biochem.*, **55**, 397–425.
Ames, G.F.-L., Prody, C. and Kutsu, S. (1984) *J. Bacteriol.*, **160**, 1181–1183.
Bax, A., Griffey, R.H. and Hawkins, B.L. (1983) *J. Magn. Reson.*, **55**, 301–315.
Bendall, M.R., Pegg, D.T. and Dodrell, D.M. (1983) *J. Magn. Reson.*, **52**, 81–117.
Bystrov, V.F. (1976) *Prog. NMR Spectrosc.*, **10**, 41–81.
Clore, M., Kay, L.E., Bax, A. and Gronenborn, A.M. (1991) *Biochemistry*, **30**, 12–18.
Drapeau, G.R., Brammar, W.J. and Yanofsky, C. (1968) *J. Mol. Biol.*, **35**, 357–367.
Driscoll, P.C., Clore, G.M., Marion, D., Wingfield, P.T. and Gronenborn, A.M. (1990) *Biochemistry*, **29**, 3542–3556.
Gilliland, G.L. and Quiocho, F.A. (1981) *J. Mol. Biol.*, **146**, 341–362.
Gronenborn, A.M., Bax, A., Wingfield, P.T. and Clore, G.M. (1989) *FEBS Lett.*, **243**, 93–98.
Hunt, A.G. and Hong, J.-S. (1981) *J. Biol. Chem.*, **256**, 11988–11991.
Hunt, A.G. and Hong, J.-S. (1983) *Biochemistry*, **22**, 851–854.
Ikura, M., Kay, L.E. and Bax, A. (1990) *Biochemistry*, **29**, 4659–4667.
Jardetzky, O. and Roberts, G.C.K. (1981) *N.M.R. in Molecular Biology*, Academic Press, New York.
Kay, L.E., Ikura, M., Tschudin, R. and Bax, A. (1990) *J. Magn. Reson.*, **89**, 496–514.
Kreishman, G.P., Robertson, D.E. and Ho, C. (1973) *Biochem. Biophys. Res. Commun.*, **53**, 18–23.
Marion, D., Kay, L.E., Sparks, S.W., Torchia, D.A. and Bax, A. (1989a) *J. Am. Chem. Soc.*, **111**, 1515–1517.
Marion, D., Driscoll, P.C., Kay, L.E., Wingfield, P.T., Bax, A., Gronenborn, A.M. and Clore, G.M. (1989b) *Biochemistry*, **28**, 6150–6156.
Montelione, G.T. and Wagner, G. (1990) *J. Magn. Reson.*, **87**, 183–188.
Mueller, L. (1979) *J. Am. Chem. Soc.*, **101**, 4481–4484.
Nohno, T., Saito, T. and Hong, J.-S. (1986) *Mol. Gen. Genet.*, **205**, 260–269.
Oh, B.H., Westler, W.M., Darba, P. and Markley, J.L. (1988) *Science*, **240**, 908–911.
Pflugrath, J.W. and Quiocho, F.A. (1988) *J. Mol. Biol.*, **200**, 163–180.
Plateau, P., Dumas, C. and Gueron, M. (1983) *J. Magn. Reson.*, **54**, 46–53.
Quiocho, F.A. and Vyas, N.K. (1984) *Nature*, **310**, 381–386.
Saper, M.A. and Quiocho, F.A. (1983) *J. Biol. Chem.*, **258**, 11057–11062.
Shen, Q., Simplaceanu, V., Cottam, P.F. and Ho, C. (1989a) *J. Mol. Biol.*, **210**, 849–857.
Shen, Q., Simplaceanu, V., Cottam, P.F., Wu, J.-L., Hong, J.-S. and Ho, C. (1989b) *J. Mol. Biol.*, **210**, 859–867.
States, D.J., Haberkorn, R.A. and Ruben, D.J. (1982) *J. Magn. Reson.*, **48**, 286–292.
Tabor, S. and Richardson, C.C. (1985) *Proc. Natl. Acad. Sci. U.S.A.*, **82**, 1074–1078.
Wagner, G. (1983) *Quart. Rev. Biophys.*, **16**, 1–57.
Weiner, J.H. and Heppel, L.A. (1971) *J. Biol. Chem.*, **246**, 6933–6941.
Westler, W.M., Kainosho, M., Nagao, H., Tomonaga, N. and Markley, J.L. (1988) *J. Am. Chem. Soc.*, **110**, 4093–4095.
Wüthrich, K. (1986) *NMR of Proteins and Nucleic Acids*, John Wiley and Sons, Inc., New York.